

# Decaying Dark Matter and the PAMELA Anomaly

Alejandro Ibarra and David Tran\*

*Physik-Department T30d, Technische Universität München,  
James-Frank-Straße, 85748 Garching, Germany.*

## Abstract

Astrophysical and cosmological observations do not require the dark matter particles to be absolutely stable. If they are indeed unstable, their decay into positrons might occur at a sufficiently large rate to allow the indirect detection of dark matter through an anomalous contribution to the cosmic positron flux. In this paper we discuss the implications of the excess in the positron fraction recently reported by the PAMELA collaboration for the scenario of decaying dark matter. To this end, we have performed a model-independent analysis of possible signatures by studying various decay channels in the case of both a fermionic and a scalar dark matter particle. We find that the steep rise in the positron fraction measured by PAMELA at energies larger than 10 GeV can naturally be accommodated in several realizations of the decaying dark matter scenario.

November 2008

---

\*E-mail addresses: [alejandro.ibarra@ph.tum.de](mailto:alejandro.ibarra@ph.tum.de), [david.tran@ph.tum.de](mailto:david.tran@ph.tum.de)

# 1 Introduction

The spallation of primary cosmic-ray protons and other nuclei on the interstellar medium produces a flux of secondary positrons which is expected to decrease monotonically with the energy [1]. Interestingly, measurements of cosmic-ray positrons undertaken by a series of experiments over the last twenty years, HEAT [2], CAPRICE [3], MASS [4] and AMS-01 [5], indicated the existence of an excess of positrons at energies above 7 GeV with respect to the expectations from a purely secondary component. The discovery of this excess raised a lot of interest among the particle physics and astrophysics communities, which interpreted the excess as a possible indirect signature of dark matter.

If dark matter particles are weakly interacting, they annihilate in the center of our Galaxy, producing a primary flux of positrons. This possibility has been extensively discussed over the last years as a potential explanation of the HEAT anomaly, although typically large boost factors have to be invoked in order to achieve sufficiently high fluxes [6–8].

Nevertheless, dark matter self-annihilation is not the only possibility for the indirect detection of the dark matter. Strictly speaking, the viability of a particle as a dark matter candidate does not require its absolute stability, but merely that the dark matter lifetime is longer than the age of the Universe. Then, if the dark matter decays proceed at a sufficiently high rate, the decay products might be detectable. There are in fact some physically well-motivated dark matter candidates which decay with very long lifetimes. For instance, gravitino dark matter which is unstable due to a small breaking of  $R$ -parity constitutes a very interesting scenario that leads to a thermal history of the Universe consistent with the observed abundances of the primordial elements, the observed dark matter relic abundance and the observed baryon asymmetry [9]. The late decays of dark matter gravitinos produce a flux of gamma rays [10,11], positrons [12,11], antiprotons [12] and neutrinos [13] which contribute to the total fluxes received at the Earth. Remarkably, it has been pointed out that the EGRET anomaly in the extragalactic gamma-ray background [14] and the HEAT excess in the positron fraction [2] can be simultaneously explained by the decay of dark matter gravitinos with a mass  $m \sim 150$  GeV and a lifetime  $\tau \sim 10^{26}$  s [12,11]. Other candidates for decaying dark matter with electroweak masses include hidden

gauge bosons [15], hidden gauginos [16], right-handed sneutrinos in  $R$ -parity breaking scenarios [17] or baryonic bound states of messenger quarks [18].

Very recently, the PAMELA collaboration [19] has published measurements of the cosmic-ray positron fraction performed with unprecedented accuracy [20]. These measurements have not only confirmed a significant deviation with respect to the expectations from a purely secondary component, but have also provided evidence for a very sharp rise of the spectrum at energies 7 – 100 GeV. In view of the new results, it is important to study whether the scenario of decaying dark matter is consistent with the energy spectrum measured by PAMELA and what constraints the new data impose on the nature of decaying dark matter. It should be borne in mind, though, that the astrophysical uncertainties in the determination of the secondary positron component are still large [21] and that nearby astrophysical sources such as pulsars might produce sizable positron fluxes in the energy range explored by PAMELA [22].

In order to keep the analysis as model-independent as possible, we will analyze the cases that the dark matter particle is either a fermion or a scalar, and we will compute the predictions for the positron fraction for various decay channels and different dark matter masses and lifetimes. Namely, in the case of a fermionic dark matter particle  $\psi$ , we will consider the two-body decay channels  $\psi \rightarrow Z^0 \nu, \psi \rightarrow W^\pm \ell^\mp$ , as well as the three-body decay channels  $\psi \rightarrow \ell^+ \ell^- \nu$ , with  $\ell = e, \mu, \tau$  being the charged leptons. On the other hand, for a scalar dark matter particle  $\phi$ , we will consider the two-body decay channels,  $\phi \rightarrow Z^0 Z^0, \phi \rightarrow W^+ W^-, \phi \rightarrow \ell^+ \ell^-$ .

This paper is organized as follows: in Section 2 we will review the propagation of positrons in the Galaxy. In Section 3 we will present our results for the positron fraction expected from the decay of a fermionic or a scalar dark matter particle and we will discuss the sensitivity of the results to the choice of the propagation model. Lastly, in Section 4 we will present our conclusions.

## 2 Positron Propagation

Positron propagation in the Milky Way is commonly described by a stationary two-zone diffusion model with cylindrical boundary conditions [23]. Under this approximation, the number density of positrons per unit energy,  $f_{e^+}(E, \vec{r}, t)$ , satisfies the following

transport equation:

$$0 = \frac{\partial f_{e+}}{\partial t} = \nabla \cdot [K(E, \vec{r}) \nabla f_{e+}] + \frac{\partial}{\partial E} [b(E, \vec{r}) f_{e+}] + Q_{e+}(E, \vec{r}) , \quad (1)$$

where convection and annihilations in the Galactic disk are neglected. The boundary conditions require the solution  $f_{e+}(E, \vec{r}, t)$  to vanish at the boundary of the diffusion zone, which is approximated by a cylinder with half-height  $L = 1 - 15$  kpc and radius  $R = 20$  kpc.

The first term on the right-hand side of the transport equation is the diffusion term, which accounts for the propagation of positrons through the tangled Galactic magnetic fields. The diffusion coefficient  $K(E, \vec{r})$  is assumed to be constant throughout the diffusion zone and is parametrized by:

$$K(E) = K_0 \beta \mathcal{R}^\delta , \quad (2)$$

where  $\beta = v/c$  is the velocity and  $\mathcal{R}$  is the rigidity of the particle, which is defined as the momentum in GeV per unit charge,  $\mathcal{R} \equiv p(\text{GeV})/Z$ . The normalization  $K_0$  and the spectral index  $\delta$  of the diffusion coefficient are related to the properties of the interstellar medium and can be determined from flux measurements of other cosmic-ray species, mainly from the Boron-to-Carbon (B/C) ratio [24]. We list in Table 1 the diffusion parameters for the propagation models M2, MED and M1 proposed in [25], which are consistent with the observed B/C ratio. The second term accounts for energy losses due to inverse Compton scattering on starlight and the cosmic microwave background, as well as synchrotron radiation and ionization. The rate of energy loss,  $b(E, \vec{r})$ , is assumed to be a spatially constant function parametrized by  $b(E) = \frac{E^2}{E_0 \tau_E}$ , with  $E_0 = 1$  GeV and  $\tau_E = 10^{16}$  s. Lastly,  $Q_{e+}(E, \vec{r})$  is the source term of positrons from the decay of a dark matter particle with mass  $m_{\text{DM}}$  and lifetime  $\tau_{\text{DM}}$ :

$$Q_{e+}(E, \vec{r}) = \frac{\rho_{\text{DM}}(\vec{r})}{m_{\text{DM}} \tau_{\text{DM}}} \frac{dN_{e+}(E)}{dE} , \quad (3)$$

where  $dN_{e+}/dE$  is the energy spectrum of positrons produced in the decay and  $\rho_{\text{DM}}(\vec{r})$  is the density profile of dark matter in our Galaxy. For our numerical analysis, we will adopt the spherically symmetric Navarro, Frenk and White (NFW) profile [26]:

$$\rho_{\text{DM}}(r) = \frac{\rho_0}{(r/r_c)[1 + (r/r_c)]^2} , \quad (4)$$

with  $\rho_0 = 0.26$  GeV/cm<sup>3</sup> and  $r_c = 20$  kpc. The normalization is chosen such that the local halo density is  $\rho_{\text{DM}}(r_\odot) = 0.3$  GeV/cm<sup>3</sup> with  $r_\odot = 8.5$  kpc [27].

Model	$\delta$	$K_0$ (kpc <sup>2</sup> /Myr)	$L$ (kpc)
M2	0.55	0.00595	1
MED	0.70	0.0112	4
M1	0.46	0.0765	15

Table 1: Diffusion parameters for the propagation models M2, MED and M1 proposed in [25] which are consistent with the observed B/C ratio.

The solution of the transport equation at the Solar System,  $r = r_\odot$ ,  $z = 0$ , can be formally expressed by the convolution

$$f_{e^+}(E) = \frac{1}{m_{\text{DM}}\tau_{\text{DM}}} \int_0^{m_{\text{DM}}} dE' G_{e^+}(E, E') \frac{dN_{e^+}(E')}{dE'}. \quad (5)$$

The solution is thus factorized into two parts. The first part, given by the Green's function  $G(E, E')$ , encodes all of the information about the astrophysics (such as the details of the halo profile and the complicated propagation of positrons in the Galaxy) and is universal for any decaying dark matter candidate. The remaining part depends exclusively on the nature and properties of the decaying dark matter candidate, namely the mass, the lifetime and the energy spectrum of positrons produced in the decay. In the next Section we will analyze several phenomenological scenarios of decaying dark matter and discuss their viability in view of the PAMELA data.

The explicit form of the Green's function is [8]

$$G_{e^+}(E, E') = \sum_{n,m=1}^{\infty} B_{nm}(E, E') J_0 \left( \zeta_n \frac{r_\odot}{R} \right) \sin \left( \frac{m\pi}{2} \right), \quad (6)$$

where  $J_0$  is the zeroth-order Bessel function of the first kind, whose successive zeros are denoted by  $\zeta_n$ . On the other hand,

$$B_{nm}(E, E') = \frac{\tau_E E_0}{E^2} C_{nm} \exp \left\{ \left( \frac{\zeta_n^2}{R^2} + \frac{m^2 \pi^2}{4L^2} \right) \frac{K_0 \tau_E}{\delta - 1} \left[ \left( \frac{E}{E_0} \right)^{\delta-1} - \left( \frac{E'}{E_0} \right)^{\delta-1} \right] \right\}, \quad (7)$$

with

$$C_{nm} = \frac{2}{J_1^2(\zeta_n) R^2 L} \int_0^R r' dr' \int_{-L}^L dz' \rho_{\text{DM}}(\vec{r}') J_0 \left( \zeta_n \frac{r'}{R} \right) \sin \left[ \frac{m\pi}{2L} (L - z') \right], \quad (8)$$

where  $J_1$  is the first-order Bessel function.

The Green's function can be well approximated by the following interpolating function, which is valid for any decaying dark matter particle [12]:

$$G_{e^+}(E, E') \simeq \frac{10^{16}}{E^2} e^{a+b(E^{\delta-1}-E'^{\delta-1})} \theta(E' - E) \text{ cm}^{-3} \text{ s}, \quad (9)$$

model	$a$	$b$
M2	-0.9716	-10.012
MED	-1.0203	-1.4493
M1	-0.9809	-1.1456

Table 2: Coefficients of the interpolating function Eq. (9) for the positron Green’s function, assuming a NFW halo profile and for the different diffusion models in Table 1.

where  $E$  and  $E'$  are expressed in units of GeV. The coefficients  $a$  and  $b$  can be found in Table 2 for the NFW profile and the different diffusion models listed in Table 1. This approximation works better than 15 – 20% over the whole range of energies. We find numerically that the Green’s function is not very sensitive to the choice of the halo profile, since the Earth receives only positrons created within a few kpc from the Sun, where the different halo profiles are very similar. Therefore, the Green’s function coefficients for other halo profiles can be well approximated by the values in Table 2.

Finally, the flux of primary positrons at the Solar System from dark matter decay is given by:

$$\Phi_{e^+}^{\text{prim}}(E) = \frac{c}{4\pi} f_{e^+}(E). \quad (10)$$

In order to compare our results with experiments, we will calculate the positron fraction, which is defined as the ratio of the total positron flux over the total electron plus positron fluxes,  $\Phi_{e^+}/(\Phi_{e^-} + \Phi_{e^+})$ . The total positron flux receives contributions from the dark matter decay as well as from a secondary component stemming from the collision of primary protons and other nuclei on the interstellar medium, which constitutes the background to any dark matter signal. On the other hand, the total electron flux has a primary astrophysical component, presumably originating from supernova remnants, a secondary component from spallation of cosmic rays on the interstellar medium, and an exotic primary component from dark matter decay that might be important at high energies in some scenarios. For the background fluxes of primary and secondary electrons, as well as secondary positrons, we will use the parametrizations

obtained in [7] from detailed computer simulations of cosmic-ray propagation [1]:

$$\Phi_{e^-}^{\text{prim}}(E) = \frac{0.16 E^{-1.1}}{1 + 11 E^{0.9} + 3.2 E^{2.15}} (\text{GeV}^{-1} \text{cm}^{-2} \text{s}^{-1} \text{sr}^{-1}) , \quad (11)$$

$$\Phi_{e^-}^{\text{sec}}(E) = \frac{0.70 E^{0.7}}{1 + 110 E^{1.5} + 600 E^{2.9} + 580 E^{4.2}} (\text{GeV}^{-1} \text{cm}^{-2} \text{s}^{-1} \text{sr}^{-1}) , \quad (12)$$

$$\Phi_{e^+}^{\text{sec}}(E) = \frac{4.5 E^{0.7}}{1 + 650 E^{2.3} + 1500 E^{4.2}} (\text{GeV}^{-1} \text{cm}^{-2} \text{s}^{-1} \text{sr}^{-1}) , \quad (13)$$

where  $E$  is the energy expressed in units of GeV.

### 3 Results

For a given model of decaying dark matter and a given propagation model, defined by the parameters in Table 1, the predictions for the positron fraction at Earth can be readily computed using the formalism explained in the previous section. To derive our results we solved the transport equation Eq. (1) numerically, although for a quick estimate of the positron fraction the interpolating function Eq. (9) may also be used.

To keep the analysis as model-independent as possible, we will analyze several possibilities for the decaying dark matter, computing the prediction for the positron fraction for either a fermionic or a bosonic particle which decays in various channels with a branching ratio of 100%. We will treat the dark matter mass and lifetime as free parameters, while the normalization of the background is kept fixed. We will first adopt the MED propagation model in order to better compare the predictions from different particle physics scenarios and later on, we will analyze the sensitivity of the predictions to the choice of the propagation model.

Let us now discuss the cases of fermionic and scalar dark matter particles separately.

In the case that the dark matter particle is a fermion  $\psi$ , the following decay channels are possible:

$$\begin{aligned} \psi &\rightarrow Z^0 \nu , \\ \psi &\rightarrow W^\pm \ell^\mp , \\ \psi &\rightarrow \ell^+ \ell^- \nu , \end{aligned} \quad (14)$$

provided that the respective channels are kinematically open.

The fragmentation of the  $Z^0$  boson in the decay  $\psi \rightarrow Z^0 \nu$  produces a continuous spectrum of positrons (mainly from  $\pi^+$  decay) that we have obtained using the

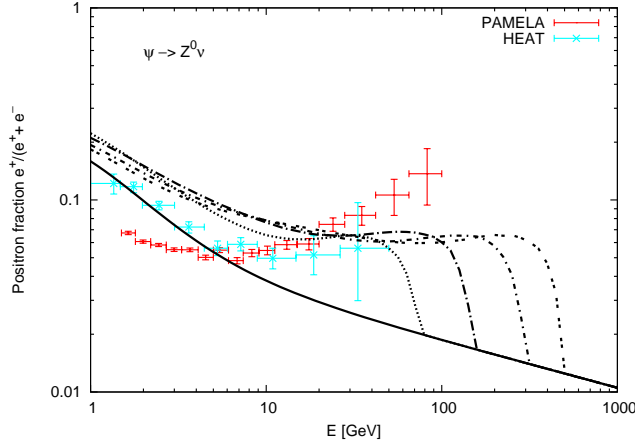


Figure 1: Positron fraction from the decay of the fermionic dark matter particle in the channel  $\psi \rightarrow Z^0 \nu$  when the dark matter mass is, from left to right,  $m_{\text{DM}} = 150, 300, 600, 1000$  GeV. The lifetime has been chosen to provide a qualitatively good fit to the data and is  $\sim 5 \times 10^{25}$  s in all the cases.

event generator PYTHIA 6.4 [28]<sup>1</sup>. The predicted positron fraction is shown in Fig. 1, compared to the PAMELA and HEAT data, for the MED propagation model and for different dark matter masses. The lifetime has been chosen in order to produce a qualitatively good fit of the prediction to the data points. We operate under the assumption that the difference between the low-energy data from HEAT and PAMELA is due to solar modulation. Therefore, we use the HEAT data at low energies, which were recorded during a period of minimum solar activity. It is apparent from the figure that this decay channel by itself cannot explain the steep rise of the spectrum observed by PAMELA for any of the masses analyzed here. We have also checked that using different propagation models does not improve the fit to the data significantly.

On the other hand, we show in Fig. 2 the prediction for the positron fraction when the fermionic dark matter particle decays as  $\psi \rightarrow W \ell$ . The positrons created in the fragmentation of the  $W$  gauge bosons produce a rather flat contribution to the positron fraction. However, the hard positrons resulting from the decay of the  $\mu$  and  $\tau$  leptons or directly from the dark matter decay into positrons produce a rise in the spectrum, which is most prominent in the decay mode  $\psi \rightarrow W^\pm e^\mp$ , although it is also

<sup>1</sup>The fragmentation of the weak gauge bosons also produces fluxes of primary antiprotons and gamma-rays, which are severely constrained by the PAMELA [29] and EGRET [30] experiments, respectively. The predictions for the antiproton and the gamma-ray fluxes of the phenomenological scenarios studied in this paper will be presented elsewhere [31].



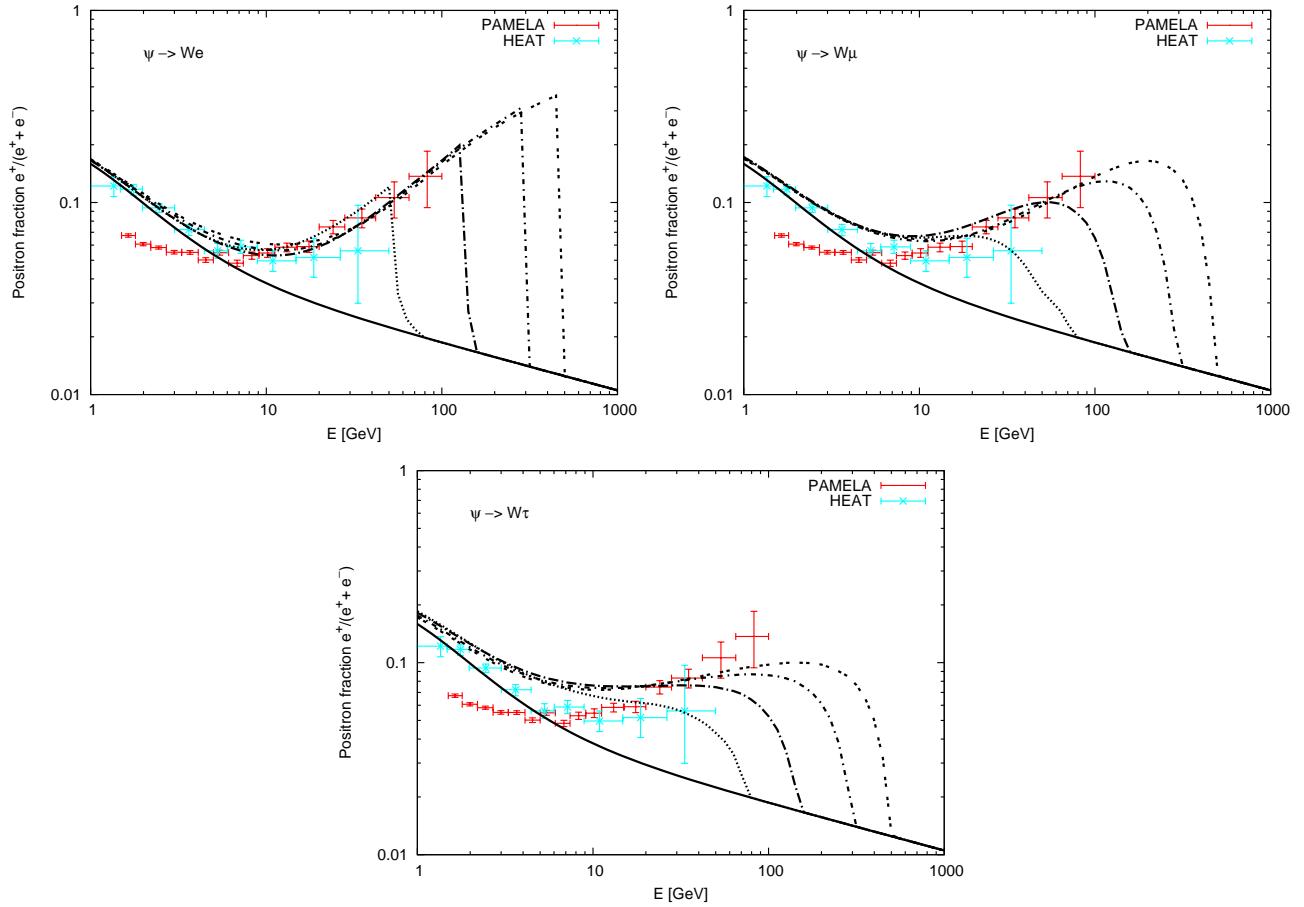


Figure 2: Positron fraction from the decay of the fermionic dark matter particle in the channels  $\psi \rightarrow W^\pm e^\mp$  (top-left panel),  $\psi \rightarrow W^\pm \mu^\mp$  (top-right panel) and  $\psi \rightarrow W^\pm \tau^\mp$  (bottom panel), when the dark matter mass is, from left to right,  $m_{\text{DM}} = 150, 300, 600, 1000$  GeV. The lifetime, which ranges between  $10^{26}$  s and  $5 \times 10^{26}$  s, is different in each case and has been chosen to provide a qualitatively good fit to the data.

quite visible in  $\psi \rightarrow W^\pm \mu^\mp$ . Interestingly, these two decay models can qualitatively reproduce the energy spectrum measured by PAMELA for dark matter masses larger than  $\sim 300$  GeV. Future measurements of the positron fraction at energies 100 – 300 GeV, as planned by the PAMELA collaboration, will be crucial to discriminate among these possibilities. Note that when the dark matter mass is large, the positron fraction in the scenario with direct decay into positrons,  $\psi \rightarrow W^\pm e^\mp$ , can reach values as large as 30 – 40%. In this case, not only the positron flux, but also the *electron* flux will receive a significant primary contribution from dark matter decay.

Lastly, we have also analyzed the case that the dark matter particle decays leptonically in a three-body decay,  $\psi \rightarrow \ell^+ \ell^- \nu$ ; the results are shown in Fig. 3. The decay

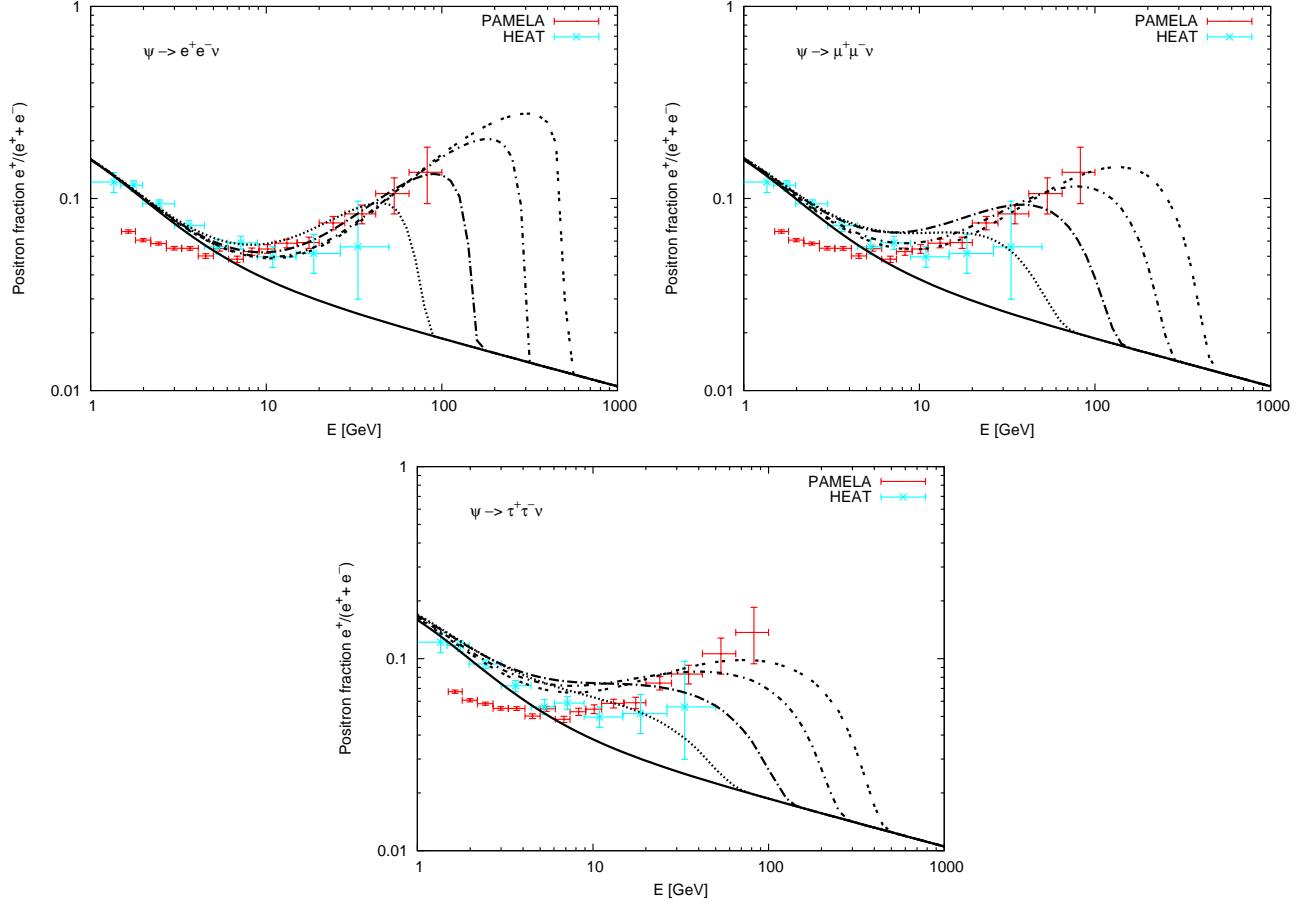


Figure 3: Positron fraction from the decay of the fermionic dark matter particle in the channels  $\psi \rightarrow e^+e^-\nu$  (top-left panel),  $\psi \rightarrow \mu^+\mu^-\nu$  (top-right panel) and  $\psi \rightarrow \tau^+\tau^-\nu$  (bottom panel), when the dark matter mass is, from left to right,  $m_{\text{DM}} = 150, 300, 600, 1000$  GeV. The lifetime, which ranges between  $5 \times 10^{25}$  s and  $8 \times 10^{26}$  s, is different in each case and has been chosen to provide a qualitatively good fit to the data.

$\psi \rightarrow e^+e^-\nu$  can explain the PAMELA anomaly when the dark matter mass is larger than  $\sim 300$  GeV, while the decay channel  $\psi \rightarrow \mu^+\mu^-\nu$  requires larger masses. In contrast, the energy spectrum produced in the decay  $\psi \rightarrow \tau^+\tau^-\nu$ , although it exhibits a notable bump, is too flat to explain the observations by itself. In this case, other contributions to the positron flux should be invoked, for instance from pulsars, in order to reproduce the observations.

When the decaying dark matter particle is a scalar, the following decay modes are

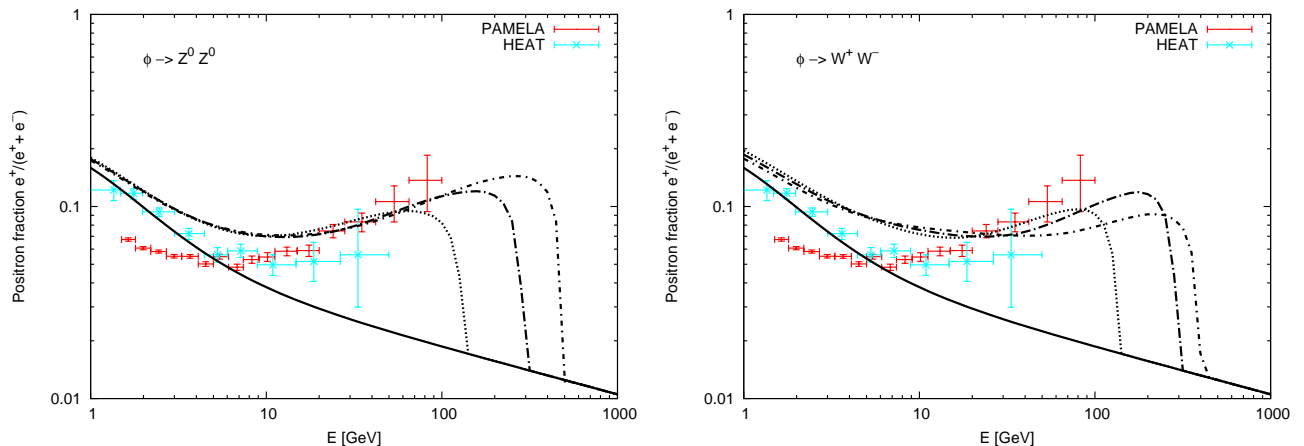


Figure 4: Positron fraction from the decay of a scalar dark matter particle in the channels  $\phi \rightarrow Z^0 Z^0$  (top-left panel) and  $\phi \rightarrow W^+ W^-$  (top-right panel) when the dark matter mass is, from left to right,  $m_{\text{DM}} = 300, 600, 1000$  GeV. The lifetime has been chosen to provide a qualitatively good fit to the data and is  $\sim 2 \times 10^{26}$  s ( $\sim 10^{26}$  s) for the decay into  $Z$  ( $W$ ) bosons.

possible:

$$\begin{aligned}
 \phi &\rightarrow Z^0 Z^0 \\
 \phi &\rightarrow W^+ W^-, \\
 \phi &\rightarrow \ell^+ \ell^-,
 \end{aligned} \tag{15}$$

again provided that the decays are kinematically open.

We show in Fig. 4 the expected positron fraction from the decay of a scalar particle into weak gauge bosons,  $\phi \rightarrow Z^0 Z^0$  or  $\phi \rightarrow W^+ W^-$ . In these decay modes, no hard lepton is produced. Instead, only positrons from the fragmentation of the weak gauge bosons will contribute. As a result, the spectral shape of the positron fraction is too flat to explain the steep rise observed by PAMELA by itself.

We have also calculated the predictions for the positron fraction when the scalar dark matter decays directly into two charged leptons,  $\phi \rightarrow \ell^+ \ell^-$ ; the results are shown in Fig. 5. The predictions are qualitatively very similar to the ones in the scenario where a dark matter fermion decays into  $W^\pm \ell^\mp$ , the most noticeable difference being the larger cutoff in the energy spectrum in the scalar case, for the same dark matter mass. To be more precise, in the scenario with  $\psi \rightarrow W^\pm \ell^\mp$  the cutoff is at  $m_{\text{DM}}/2(1 - M_W^2/m_{\text{DM}}^2)$  while in the scenario with  $\phi \rightarrow \ell^+ \ell^-$ , it is at the larger value

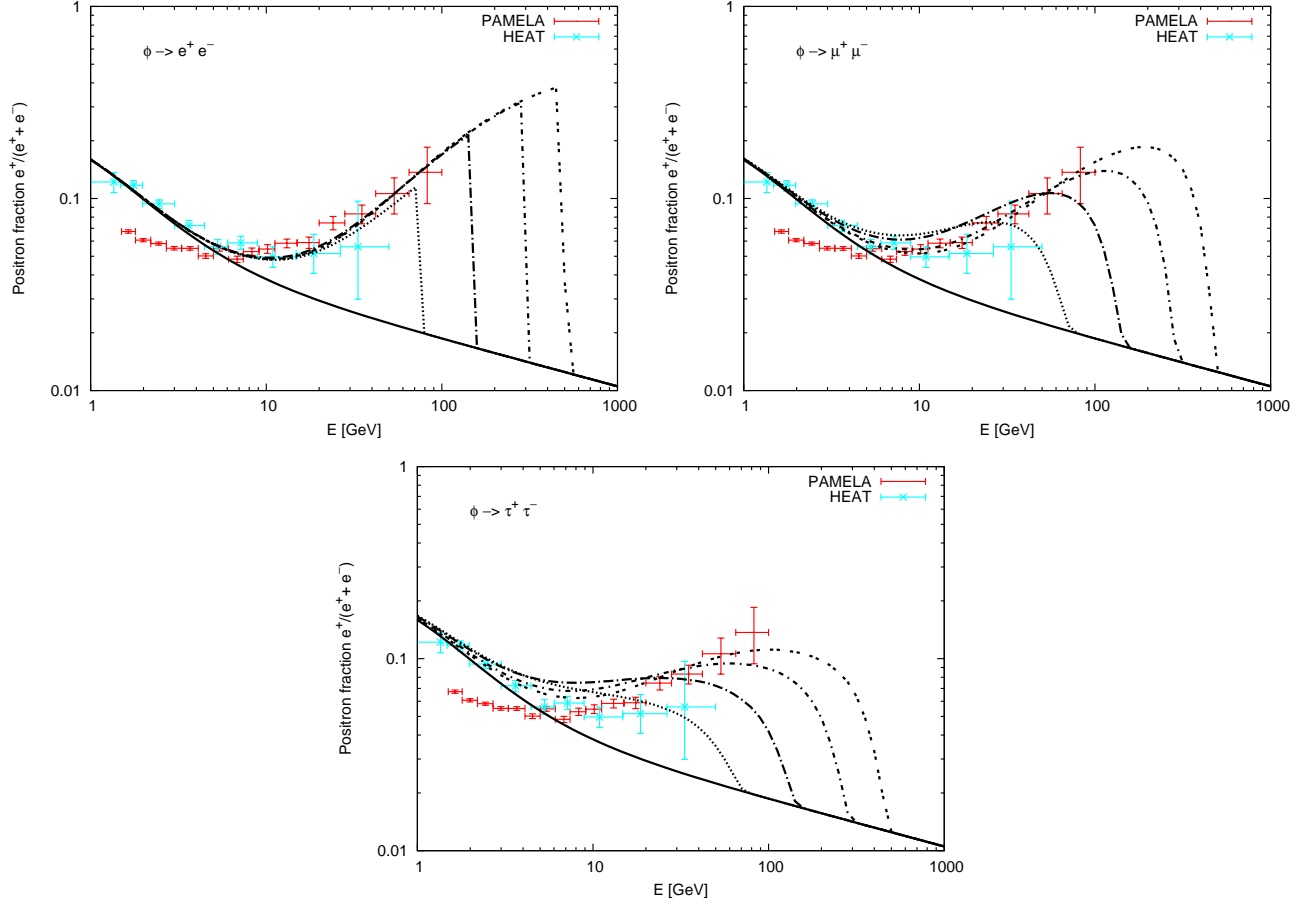


Figure 5: Positron fraction from the decay of a scalar dark matter particle in the channels  $\phi \rightarrow e^+e^-$  (top-left panel),  $\phi \rightarrow \mu^+\mu^-$  (top-right panel) and  $\phi \rightarrow \tau^+\tau^-$  (bottom panel), when the dark matter mass is, from left to right,  $m_{\text{DM}} = 150, 300, 600, 1000$  GeV. The lifetime, which ranges between  $10^{26}$  s and  $10^{27}$  s, is different in each case and has been chosen to provide a qualitatively good fit to the data.

$m_{\text{DM}}/2$ . For this class of scenarios, the decay modes into positrons or antimuons can accommodate the PAMELA anomaly better than the decay mode into antitau.

Above we have analyzed the predictions for the positron fraction for different scenarios of fermionic or scalar decaying dark matter, assuming the MED propagation model. After discussing the sensitivity of the predictions to the choice of the particle physics model, we would like to briefly address the sensitivity of the results to astrophysical uncertainties.

We show in Fig. 6 the sensitivity to the propagation model of four particle physics scenarios consisting of a dark matter fermion which decays into two particles,  $\psi \rightarrow$

$W^\pm(e, \mu)^\mp$ , or into three particles,  $\psi \rightarrow (e, \mu)^+(e, \mu)^-\nu$ . These scenarios are characterized by the direct decay into hard positrons or antimuons, and were found to be compatible with the excess observed by PAMELA for the MED propagation model. The results in Fig. 6 show that this conclusion still holds for the M1 and M2 propagation models: the M1 and MED propagation models yield very similar predictions of the positron fraction, while the M2 propagation model yields a slightly larger positron fraction at high energies and a smaller positron fraction at low energies. The reason is that in the M2 propagation model the diffusion is minimal and thus the hard spectrum of injected positrons from dark matter decay is less altered by the propagation than in the MED and M1 model, yielding a steeper rise in the positron fraction measured at Earth. The same conclusion holds for the scenarios where a scalar dark matter particle directly decays into an electron-positron pair or a muon-antimuon pair,  $\phi \rightarrow (e, \mu)^+(e, \mu)^-$ , which as discussed above yield very similar signatures in the positron fraction as the scenarios with fermionic dark matter  $\psi \rightarrow W^\pm(e, \mu)^\mp$ , where the dark matter also decays into a monoenergetic positron or antimuon.

As a last remark, let us note that the origin of the positron excess might not be the decay of the dark matter itself, but the decay of another long-lived particle which is present in our Galaxy. Notice that in the scenarios analyzed in this paper with decaying dark matter, the shape of the spectrum is determined by the dark matter mass, while the normalization, by the combination  $\rho_{\text{DM}}(r_\odot)/\tau_{\text{DM}}$ , with  $\rho_{\text{DM}}(r_\odot) = 0.3 \text{ GeV/cm}^3$  being the local density of dark matter particles (*cf.* Eqs. (3,4)). Therefore, identical signatures in the positron fraction are obtained if the decaying particle has a mass  $m'$ , a lifetime  $\tau'$  and a local abundance  $\rho'(r_\odot)$  satisfying<sup>2</sup>

$$\begin{aligned} m' &= m_{\text{DM}} , \\ \rho'(r_\odot)/\tau' &= \rho_{\text{DM}}(r_\odot)/\tau_{\text{DM}} . \end{aligned} \tag{16}$$

This opens new possibilities for model building. For instance, it is conceivable that the dominant component of dark matter is completely stable (perhaps even annihilating), while the origin of the positron excess is the decay of a subdominant form of dark matter.

---

<sup>2</sup>We assume here that any weakly or superweakly interacting particle with a lifetime longer than the age of the Universe is present in our Galaxy and has a halo distribution identical to the dominant component of dark matter.

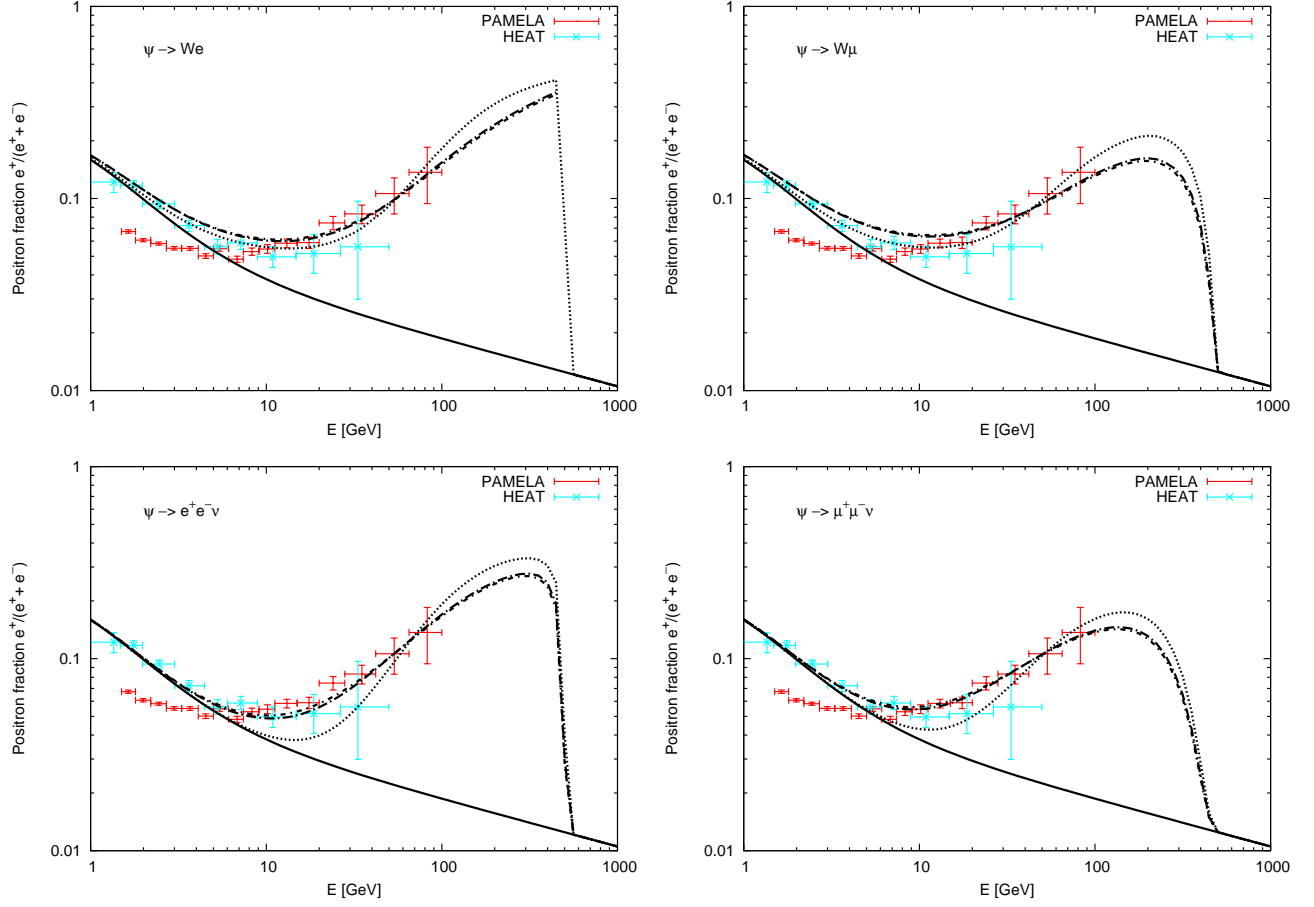


Figure 6: Dependence of the predicted positron fraction on the propagation model. For a decaying dark matter fermion with  $m_{\text{DM}} = 1000$  GeV, we show the decay modes  $\psi \rightarrow W^\pm e^\mp$  (top-left panel),  $\psi \rightarrow W^\pm \mu^\mp$  (top-right panel),  $\psi \rightarrow e^+ e^- \nu$  (bottom-left panel),  $\psi \rightarrow \mu^+ \mu^- \nu$  (bottom-right panel). The dotted line corresponds to the M2 propagation model, while the almost indistinguishable dashed-dotted lines correspond to the MED and the M1 models (see Table 1).

## 4 Conclusions

We have computed the predictions for the positron fraction of several decaying dark matter scenarios and discussed their viability in view of the new measurements reported by the PAMELA collaboration. We have studied scenarios where the dark matter particle is a fermion  $\psi$ , which decays in the two-body decay channels  $\psi \rightarrow Z^0 \nu$ ,  $W^\pm \ell^\mp$  or in the three-body decay channel  $\psi \rightarrow \ell^+ \ell^- \nu$ , where  $\ell = e, \mu, \tau$  denotes the charged leptons. In addition, we have also studied scenarios where the dark matter particle is a scalar  $\phi$ , which decays as  $\phi \rightarrow Z^0 Z^0$ ,  $\phi \rightarrow W^+ W^-$ ,  $\phi \rightarrow \ell^+ \ell^-$ .

We have found that decay channels producing hard positrons and antimuons are favored by the PAMELA data. Namely, the decay channels of a fermionic dark matter particle  $\psi \rightarrow W(\mu, e)$  and  $\psi \rightarrow (\mu, e)^+(\mu, e)^-\nu$ , and the decay channels of a scalar dark matter particle  $\phi \rightarrow (\mu, e)^+(\mu, e)^-$  produce a steep rise in the positron fraction above 10 GeV, as observed by the PAMELA collaboration. It is worth noting that the spectral shape of the positron fraction resulting from a sharply peaked positron or antimuon injection spectrum matches the experimental results quite accurately. On the other hand, decay modes involving the tau lepton can contribute to an excess in the positron fraction at high energies, although the resulting spectrum is too flat. Finally, the decay of a scalar particle into weak gauge bosons,  $\phi \rightarrow Z^0 Z^0$ ,  $\phi \rightarrow W^+ W^-$ , can also contribute to an excess in the positron fraction, although the spectrum is also too flat to fit the PAMELA data by itself. In addition, these decay channels are also disfavored by antiproton overproduction constraints for dark matter lifetimes that yield appreciable contributions to the positron flux.

If dark matter decay is indeed the primary cause for the observed positron excess, the PAMELA data clearly seem to point toward a rather heavy dark matter particle,  $m_{\text{DM}} \gtrsim 300$  GeV, which preferentially decays directly into first or second generation charged leptons with a lifetime  $\tau_{\text{DM}} \sim 10^{26}$  s.

Future measurements of the positron fraction in the energy range 100 – 300 GeV by PAMELA will provide invaluable information about scenarios with decaying dark matter and the properties of the decaying particles. Furthermore, the constraints on the predicted antiproton flux by these same scenarios from PAMELA [29] and on the gamma-ray flux from EGRET [30] (and in the near future from the Fermi Gamma-ray Space Telescope [32]) offer complementary information about this scenario, which will be presented elsewhere [31].

## Note Added

During the completion of this work two preprints appeared presenting related analyses [33,34].

## References

- [1] I. V. Moskalenko and A. W. Strong, *Astrophys. J.* **493** (1998) 694.

- [2] S. W. Barwick *et al.* [HEAT Collaboration], *Astrophys. J.* **482** (1997) L191.
- [3] M. Boezio *et al.* [CAPRICE Collaboration], *Astrophys. J.* **532** (2000) 653.
- [4] C. Grimani *et al.*, *Astron. Astrophys.* **392** (2002) 287.
- [5] M. Aguilar *et al.* [AMS-01 Collaboration], *Phys. Lett. B* **646**, 145 (2007).
- [6] A. J. Tylka, *Phys. Rev. Lett.* **63** (1989) 840 [Erratum-ibid. **63** (1989) 1658];  
M. S. Turner and F. Wilczek, *Phys. Rev. D* **42** (1990) 1001; M. Kamionkowski  
and M. S. Turner, *Phys. Rev. D* **43** (1991) 1774; G. L. Kane, L. T. Wang and  
J. D. Wells, *Phys. Rev. D* **65** (2002) 057701; E. A. Baltz, J. Edsjo, K. Freese  
and P. Gondolo, *Phys. Rev. D* **65** (2002) 063511; G. L. Kane, L. T. Wang  
and T. T. Wang, *Phys. Lett. B* **536** (2002) 263; H. C. Cheng, J. L. Feng and  
K. T. Matchev, *Phys. Rev. Lett.* **89**, 211301 (2002); D. Hooper and G. D. Kribs,  
*Phys. Rev. D* **70** (2004) 115004; M. Cirelli, R. Franceschini and A. Strumia, *Nucl.*  
*Phys. B* **800** (2008) 204.
- [7] E. A. Baltz and J. Edsjo, *Phys. Rev. D* **59** (1999) 023511.
- [8] J. Hisano, S. Matsumoto, O. Saito and M. Senami, *Phys. Rev. D* **73** (2006) 055004.
- [9] W. Buchmüller, L. Covi, K. Hamaguchi, A. Ibarra and T. Yanagida, *JHEP* **0703**,  
037 (2007).
- [10] A. Ibarra and D. Tran, *Phys. Rev. Lett.* **100**, 061301 (2008).
- [11] K. Ishiwata, S. Matsumoto and T. Moroi, arXiv:0805.1133 [hep-ph].
- [12] A. Ibarra and D. Tran, *JCAP* **0807** (2008) 002.
- [13] L. Covi, M. Grefe, A. Ibarra and D. Tran, arXiv:0809.5030 [hep-ph].
- [14] A. W. Strong, I. V. Moskalenko and O. Reimer, *Astrophys. J.* **613** (2004) 962;  
*Astrophys. J.* **613** (2004) 956.
- [15] C. R. Chen, F. Takahashi and T. T. Yanagida, arXiv:0809.0792 [hep-ph];  
arXiv:0811.0477 [hep-ph].
- [16] A. Ibarra, A. Ringwald and C. Weniger, arXiv:0809.3196 [hep-ph].



- [17] C. R. Chen and F. Takahashi, arXiv:0810.4110 [hep-ph].
- [18] K. Hamaguchi, E. Nakamura, S. Shirai and T. T. Yanagida, arXiv:0811.0737 [hep-ph].
- [19] P. Picozza *et al.*, Astropart. Phys. **27** (2007) 296.
- [20] O. Adriani *et al.*, arXiv:0810.4995 [astro-ph].
- [21] T. Delahaye, F. Donato, N. Fornengo, J. Lavalle, R. Lineros, P. Salati and R. Taillet, arXiv:0809.5268 [astro-ph].
- [22] A. K. Harding and R. Ramaty, Proc. 20th ICRC, Moscow **2**, 92-95 (1987); A. M. Atoian, F. A. Aharonian and H. J. Volk, Phys. Rev. D **52** (1995) 3265; X. Chi, E. C. M. Young and K. S. Cheng, Astrophys. J. **459** (1995) L83; C. Grigiani, Astron. Astrophys. **418**, 649 (2004); D. Hooper, P. Blasi and P. D. Serpico, arXiv:0810.1527 [astro-ph].
- [23] See for example V. S. Berezinskii, S. V. Buolanov, V. A. Dogiel, V. L. Ginzburg, V. S. Ptuskin, Astrophysics of Cosmic Rays (Amsterdam: North-Holland, 1990).
- [24] D. Maurin, F. Donato, R. Taillet and P. Salati, Astrophys. J. **555** (2001) 585.
- [25] T. Delahaye, R. Lineros, F. Donato, N. Fornengo and P. Salati, Phys. Rev. D **77** (2008) 063527.
- [26] J. F. Navarro, C. S. Frenk and S. D. M. White, Astrophys. J. **462** (1996) 563.
- [27] L. Bergstrom, P. Ullio and J. H. Buckley, Astropart. Phys. **9** (1998) 137.
- [28] T. Sjöstrand, S. Mrenna and P. Skands, JHEP **0605** (2006) 026.
- [29] O. Adriani *et al.*, arXiv:0810.4994 [astro-ph].
- [30] P. Sreekumar *et al.* [EGRET Collaboration], Astrophys. J. **494** (1998) 523.
- [31] In preparation.
- [32] <http://fermi.gsfc.nasa.gov/>.
- [33] P. f. Yin, Q. Yuan, J. Liu, J. Zhang, X. j. Bi and S. h. Zhu, arXiv:0811.0176 [hep-ph].

[34] K. Ishiwata, S. Matsumoto and T. Moroi, arXiv:0811.0250 [hep-ph].